

Inherent optical behavior and structural variation in $\text{Na}_{0.5}\text{Bi}_{0.5}\text{TiO}_3$ -6% BaTiO_3 revealed by temperature dependent Raman scattering and ultraviolet-visible transmittance

T. Huang, Z. G. Hu, G. S. Xu, X. L. Zhang, J. Z. Zhang, and J. H. Chu

Citation: [Applied Physics Letters](#) **104**, 111908 (2014); doi: 10.1063/1.4869309

View online: <http://dx.doi.org/10.1063/1.4869309>

View Table of Contents: <http://scitation.aip.org/content/aip/journal/apl/104/11?ver=pdfcov>

Published by the [AIP Publishing](#)

Articles you may be interested in

[Large strain response based on relaxor-antiferroelectric coherence in \$\text{Bi}_{0.5}\text{Na}_{0.5}\text{TiO}_3\$ - \$\text{SrTiO}_3\$ -\(\$\text{K}_{0.5}\text{Na}_{0.5}\$ \) \$\text{NbO}_3\$ solid solutions](#)

[J. Appl. Phys.](#) **116**, 184104 (2014); 10.1063/1.4901549

[Structural stability and depolarization of manganese-doped \(\$\text{Bi}_{0.5}\text{Na}_{0.5}\$ \) \$_{1-x}\text{Ba}_x\text{TiO}_3\$ relaxor ferroelectrics](#)

[J. Appl. Phys.](#) **116**, 154101 (2014); 10.1063/1.4898322

[Composition induced structure evolution and large strain response in ternary \$\text{Bi}_{0.5}\text{Na}_{0.5}\text{TiO}_3\$ - \$\text{Bi}_{0.5}\text{K}_{0.5}\text{TiO}_3\$ - \$\text{SrTiO}_3\$ solid solution](#)

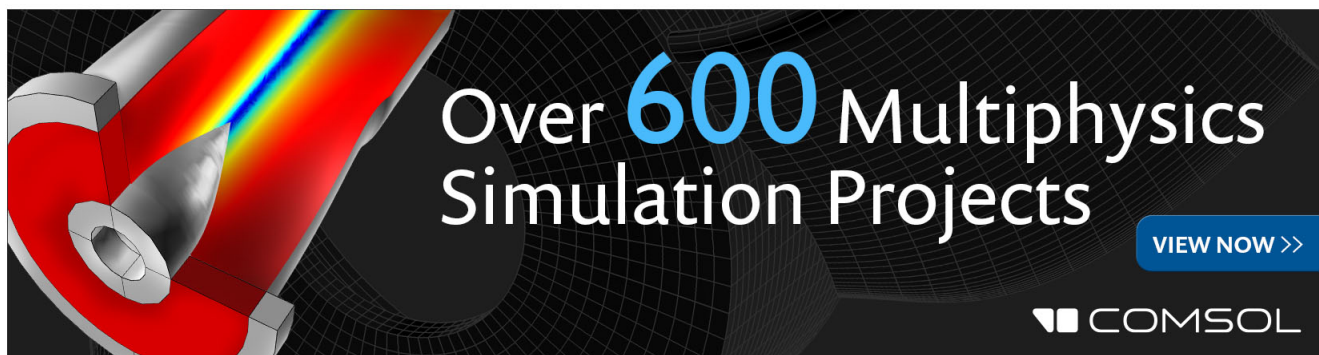
[J. Appl. Phys.](#) **114**, 164105 (2013); 10.1063/1.4825122

[Origin of large recoverable strain in \$0.94\(\text{Bi}_{0.5}\text{Na}_{0.5}\)\text{TiO}_3\$ - \$0.06\text{BaTiO}_3\$ near the ferroelectric-relaxor transition](#)

[Appl. Phys. Lett.](#) **102**, 062902 (2013); 10.1063/1.4790285

[Inference of oxygen vacancies in hydrothermal \$\text{Na}_{0.5}\text{Bi}_{0.5}\text{TiO}_3\$](#)

[Appl. Phys. Lett.](#) **101**, 142902 (2012); 10.1063/1.4755882

An advertisement for COMSOL Multiphysics. On the left, there is a 3D cutaway illustration of a mechanical part, possibly a turbine or engine component, with a rainbow-colored stress or temperature distribution overlaid. The text 'Over 600 Multiphysics Simulation Projects' is prominently displayed in the center in a large, white, sans-serif font. To the right of this text is a blue button with the text 'VIEW NOW >>'. In the bottom right corner, the COMSOL logo is visible, consisting of a small square icon followed by the word 'COMSOL' in a white, sans-serif font.

Inherent optical behavior and structural variation in $\text{Na}_{0.5}\text{Bi}_{0.5}\text{TiO}_3$ -6%BaTiO₃ revealed by temperature dependent Raman scattering and ultraviolet-visible transmittance

T. Huang (黄婷),¹ Z. G. Hu (胡志高),^{1,a)} G. S. Xu (许桂生),² X. L. Zhang (张小龙),¹ J. Z. Zhang (张金中),^{1,3} and J. H. Chu (褚君浩)^{1,3}

¹Key Laboratory of Polar Materials and Devices, Ministry of Education, Department of Electronic Engineering, East China Normal University, Shanghai 200241, China

²R&D Center of Synthetic Crystals, Shanghai Institute of Ceramics, Chinese Academy of Sciences, Shanghai 201800, China

³National Laboratory for Infrared Physics, Shanghai Institute of Technical Physics, Chinese Academy of Science, Shanghai 200083, China

(Received 26 January 2014; accepted 12 March 2014; published online 20 March 2014)

Optical properties of $\text{Na}_{0.5}\text{Bi}_{0.5}\text{TiO}_3$ -6%BaTiO₃ (NBT-6%BT) single crystal have been studied by temperature dependent Raman and ultraviolet-visible spectra from 25 to 180 °C. With increasing the temperature, the absorption edge approximately decreases from 3.13 to 3.04 eV. Moreover, abnormal changes of phonon mode and spectral transmission are observed at 83, 106, and 150 °C, which can be unambiguously correlated with thermal evolutions of polar nano-regions and phase transition. It indicates that there is an inherent relationship between optical behavior and structural variation of NBT-6%BT, which provides a valid methodology to explore the phase transition of relaxor ferroelectric oxides. © 2014 AIP Publishing LLC. [<http://dx.doi.org/10.1063/1.4869309>]

Bismuth sodium titanate $\text{Na}_{0.5}\text{Bi}_{0.5}\text{TiO}_3$ (NBT), first discovered by Smolenskii *et al.*,¹ adopts complex ABO₃ perovskite with A-site being equally shared by two different cations (Na^+ and Bi^{3+}). NBT and NBT-based compounds have been regarded as one of the future generation of environmental-friendly ferroelectric (FE) materials to replace the widely used lead-based piezoelectrics due to its large remnant polarization and relatively good piezoelectric properties.^{2,3} Among these NBT-based solid solutions, BaTiO₃ (BT) modified NBT system, $\text{Na}_{0.5}\text{Bi}_{0.5}\text{TiO}_3$ - $x\%$ BaTiO₃ (NBT- $x\%$ BT) is the most attractive and promising. NBT- $x\%$ BT emerges as potential lead-free piezoelectric systems with a rhombohedral (R) to tetragonal (T) phase transition at morphotropic phase boundary (MPB) of $6 < x < 8$.^{3,4} It was reported that NBT- $x\%$ BT near the MPB region exhibits the highest piezoelectric constants and electric field induced strains.² In view of the well established correlation between enhanced piezoelectric properties and MPB patterns, there is an increasing emphasis on lead-free ferroelectric MPB systems. As a result, NBT-6%BT is explored for its unique structure property as a prototypical bismuth-based piezoceramic in numerous fundamental studies.⁵⁻⁷ Accordingly, physical properties of NBT-6%BT material, such as electrical and optical characteristics, should be thoroughly studied for potential device applications.

As a relaxor ferroelectrics, NBT- $x\%$ BT (x is 6 and 11) has complex domain structures and undergoes a complicated phase transition sequence.⁸ Note that the phase diagram of NBT- $x\%$ BT is still uncertain at MPB region from dielectric and piezoelectric data, especially below 180 °C.⁶ In general, NBT-6%BT is considered to be stabilized in a coexistence of the rhombohedral and tetragonal structure at room temperature (RT) and over a wide range of temperatures, i.e.,

~150 °C.^{8,9} Nevertheless, the exact nature of these phases and the temperature for rhombohedral to tetragonal transition are still controversial. Recent investigations indicated that the relaxor state for the BT compositions near the MPB region coexists from polar nano-regions (PNRs) with tetragonal (P4bm, $a^0a^0c^+$ in-phase oxygen octahedral tilting¹⁰) and rhombohedral (R3c, $a^-a^-a^-$ anti-phase oxygen octahedral tilting¹⁰) symmetries within an average cubic matrix.^{5,8,9,11-13} It suggests that phase transition process of NBT-6%BT system is far away from the clarification and further investigations, especially optical properties are necessary. This is because optical responses can be directly connected with interband/intraband electronic transitions for materials studied. Therefore, optical characterizations could be complementary methodology for discovering phase transition dynamics of NBT-6%BT relaxor ferroelectrics.

The nondestructive Raman scattering is an advantageous tool to provide precise information about local distortions and ionic configurations in the crystal structures.¹⁴ Recently, Raman spectroscopy has been used to study phase transitions and the nanoscale structural characteristics of NBT-based solid solutions.^{6,15-17} However, Raman studies for NBT-based systems seldom focus on the controversial temperature range of 25–180 °C. Although dielectric, piezoelectric, ferroelectric properties, phase transition behavior, and domain structures of NBT- $x\%$ BT single crystals have been extensively studied,^{2,5,11,18} less attention has been paid to optical properties, especially temperature dependence of electronic transitions for NBT-6%BT materials. As the important macroscopic phenomena, optical properties are strongly related to the electronic structures, which can be essentially determined by crystal structures.¹⁹ Therefore, one can investigate the phase transition behavior by analyzing electronic band structures and/or dielectric functions corresponding to the lattice variation. Furthermore, spectral technique takes

^{a)}Author to whom correspondence should be addressed. Electronic mail: zghu@ee.ecnu.edu.cn. Tel.: +86-21-54345150. Fax: +86-21-54345119.

advantages of nondestructive measurement and avoiding interface effects from electrodes, etc.

In the Letter, Raman and ultraviolet-visible (UV-VIS) spectra of $\text{Na}_{0.5}\text{Bi}_{0.5}\text{TiO}_3$ -6%BaTiO₃ (NBT-6%BT) single crystal have been investigated as a function of temperature from 25 to 180 °C. The variations from the phonon mode, band gap, and transmittance have been discussed in detail. The results reveal an intrinsic relationship between optical behavior and structural variation of NBT-6%BT single crystal.

Single crystal of NBT-6%BT was grown by Bridgman method, using the appropriate amount of Na_2CO_3 , Bi_2O_3 , TiO_2 , and BaCO_3 oxide powders as starting reagents.¹⁸ The obtained crystal was cut perpendicular to the $\langle 001 \rangle$ direction. The crystal was double-side polished with a mechanical polishing process to smooth the surface. Then, the specimen was cleaned in pure ethanol with an ultrasonic bath and rinsed by deionized water for several times for spectral measurements. Note that the specimen has been annealed (~ 400 °C) after the mechanical polishing prior to spectral measurements. The normal-incident transmittance spectra were measured by a double beam ultraviolet-infrared spectrophotometer (PerkinElmer UV/VIS Lambda 950) at the wavelength region of 2650-190 nm (0.5–6.5 eV) with the interval of 2 nm. The sample was mounted on a heating stage (Bruker A511) for high temperature experiments from 25 to 180 °C with a resolution of about 0.5 °C.²⁰ Temperature dependent Raman scattering experiments were carried out by a Jobin-Yvon LabRAM HR 800 micro-Raman spectrometer and a THMSE 600 heating/cooling stage (Linkam Scientific Instruments) in the temperature range from 25 to 180 °C with a resolution of 0.1 °C. The crystal was excited by the 488 nm line of an Ar laser at power of ~ 20 mW and recorded in back-scattering geometry with a resolution of better than 1 cm^{-1} . The laser beam was focused through a $50\times$ microscope with a working distance of 18 mm. An air-cooled charge coupled device (CCD) (-70 °C) with a 1024×256 pixels front illuminated chip was used to collect the scattered signal dispersed on 1800 grooves/mm grating.¹⁴ Note that no mathematical smoothing has been performed on the experimental data.

Detailed X-ray powder diffraction (XRD) information about the specimen could refer to the previous work, which revealed the coexistence of rhombohedral and tetragonal phase in the measured crystal.¹⁸ Note that the diffraction peak intensity could be related to the domain structure, which can result in the slight discrepancy on the XRD pattern. Moreover, the X-ray fluorescence analysis shows that the actual composition of the crystal is located at about 6% (not shown). Fig. 1 depicts temperature dependent Raman spectra with its Lorentzian-shaped deconvolution at RT. The relatively broadening phonon bands can be attributed to the A-site disorder and the overlapping of Raman modes is due to the lattice anharmonicity. Four main regions can be discerned. The first one at about 135 cm^{-1} is dominated by the A_1 mode assigned to A-site cation variations and sensitive towards phase transitions in which the A-site symmetry changes.^{16,17,21} The second region at around 280 cm^{-1} is dominated by TiO_6 octahedra.^{16,17} In a general matter, it has been shown that changes in this region are not only related to polar Ti-cation displacement but also to the octahedron-tilt-related distortion, which can reflect important structural

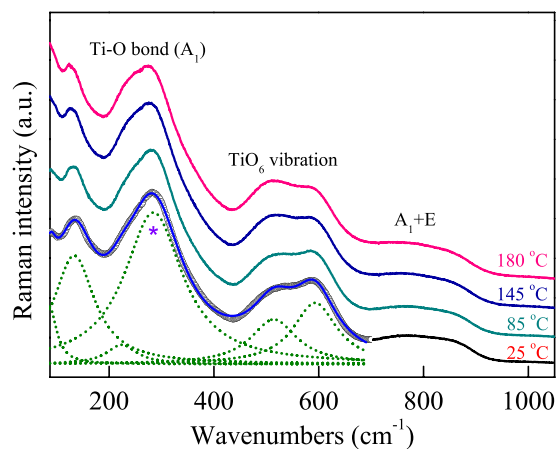


FIG. 1. Raman spectra of NBT-6%BT single crystal as a function of temperature. In order to better illustrate changes in peak characteristics with the temperature, Lorentzian-shaped spectral deconvolution is shown by the dashed lines and the symbol “*” stands for the phonon mode near 285 cm^{-1} .

variations. Therefore, this region can be used to identify phase transitions in classic and complex ferroelectrics.²¹ The third region ($450\text{--}700\text{ cm}^{-1}$) is related to oxygen octahedral variations/rotations,²¹ most likely as a superposition of transverse optical (TO) and longitudinal optical (LO) bands of the A_1 character. Besides, the region above 700 cm^{-1} has been linked to the $A_1(\text{LO})$ and $E(\text{LO})$ overlapping bands. Owing to the challenges of intrinsic broadening and overlapping of phonon modes on the assignment of mode symmetries, structural analysis thus relies on discussing soft-mode or hard-mode behavior as a function of composition, pressure, or temperature.^{6,15,17} Note that the phonon modes can be explained by the variations of frequency, intensity, and full width at half maximum (FWHM) of Raman spectra.¹⁴ Fig. 2 shows the peak and integrated intensity at 285 cm^{-1} (B-O) as a function of temperature for NBT-6%BT. Three main regions can be discerned. Each region shows an increasing/decreasing trend in both integrated intensity and phonon frequency, respectively. The B-O variations near 285 cm^{-1} are related to the ferroelectric phase transformation and soft mode.^{21,22} The negative frequency shift for this mode suggests that the particular phonon is directly involved in the phase transition. Note that two deviations from linearity for the frequency variation are observed at about 106 and 150 °C, corresponding to the changes in slope of integrated intensity well.

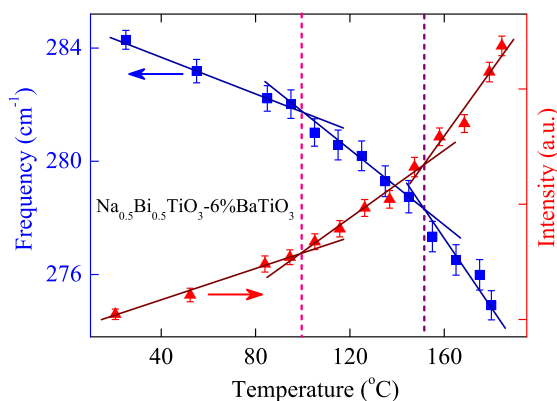


FIG. 2. Temperature dependence of phonon frequency and integrated intensities for NBT-6%BT single crystal. Note that the dashed lines indicate the temperature points for different variation trends.

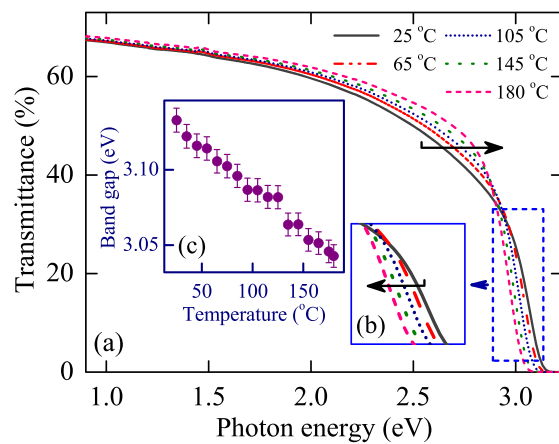


FIG. 3. (a) Transmittance spectra of NBT-6%BT single crystal at the temperatures of 25, 65, 105, 145, and 180 °C, respectively. Inset (b) shows an enlarged region near the fundamental absorption edge. Inset (c) shows that the band gap of NBT-6%BT crystal is varied with increasing the temperature.

To confirm the structural variations during the heating temperature, UV-VIS transmittance was performed. Fig. 3(a) shows the transmittance spectra of the NBT-6%BT single crystal. The absorption edge has a red shift trend with elevated temperature, which can be observed from most of semiconductors and dielectrics.¹⁹ The crystal is nearly transparent from visible to near-infrared region and the transmission decreases with increasing the temperature, down to zero in the ultraviolet region, as can be observed for most of crystals with oxygen-octahedral perovskite.²³ Fig. 3(b) exhibits an enlarged region near the direct band gap. Interestingly, the trend of the transmittance spectra in the near-infrared region is opposite to that from ultraviolet region. Note that the straight lines near the absorption edge in $(ah\nu)^2$ vs. $h\nu$ curves provide evidence for direct optical band gap, which can be obtained by extrapolating the plot $(ah\nu)^2 = 0$.²⁰ It can be seen from inset (c) that the direct band gap of the NBT-6%BT single crystal approximately decreases from 3.13 to 3.04 eV as the temperature increasing. The BO_6 (TiO_6) octahedron building block determines the basic energy level of the NBT-6%BT crystal. What is more, optical properties of oxygen-octahedral ferroelectrics are primarily controlled by the BO_6 octahedra. The B-cation d orbitals and its octahedron rule the lower lying conduction bands (CBs) while the O-anion $2p$ orbitals associated with its octahedron govern the upper valence bands (VBs).^{16,20,24} According to the results from Niranjana *et al.*,¹⁶ the states in the VB are primarily constituted of O- $2p$ states. There is a weak hybridization between O- $2p$ orbitals and Bi- $6p$ at lower energy part of the VB, as well as Ti- $3d$ orbitals in higher energy part of the VB. The states in the CB arise mainly from the Ti- $3d$ orbitals, while Bi- $6p$ states give weaker contribution. In contrast, other ions in the structure contribute to the higher-lying conduction band and have small effects. That is to say, the B-site ion has stronger influence on the refined energy level than that of the A-site.²⁰

Figs. 4(a) and 4(b) represent the transmission at the wavelength of 650 and 800 nm as a function of temperature, respectively. The transmission at the wavelength of 650 nm (about 1.91 eV) increases from 60.1% at 25 °C to 62.7% at

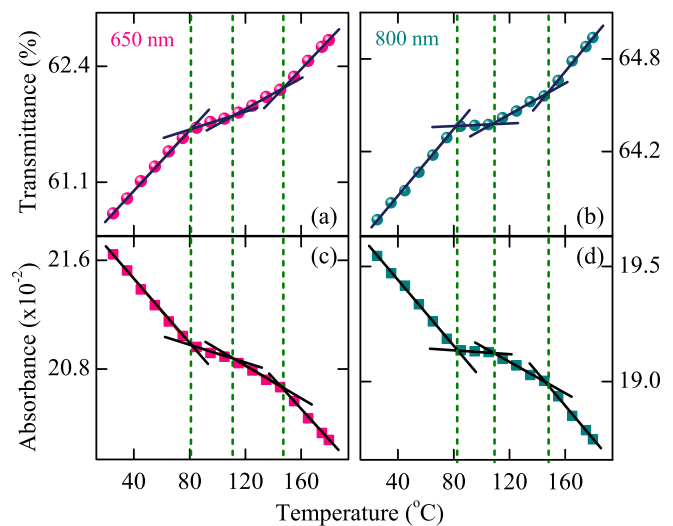


FIG. 4. Temperature dependent transmittance of NBT-6%BT crystal at the wavelength of (a) 650 nm and (b) 800 nm, respectively. Correspondingly, the parts (c) and (d) exhibit the absorbance spectra of NBT-6%BT crystal at the wavelength of 650 nm and 800 nm, respectively. Note that the dashed lines mark the discontinuity in the slope, which can be described to the structural variations. The arrows represent the trend of increasing the temperature.

180 °C, while the one at 800 nm (about 1.55 eV) increases from 63.7% at 25 °C to 65% at 180 °C. The gradually increasing transmission is due to the reduction of optical loss caused by scattering. Keep in mind that the main contributions to optical loss come from the band gap as well as domain wall scattering, which work via nanodomain wall or PNRs. The former plays an important role when the photon energy is near the band gap, while the later becomes dominant on condition that the spectral wavelength is comparable with the PNRs in length scale.²⁰ In addition, the unpoled crystal has domains with orientation of their crystallographic axes, due to their different directions of spontaneous polarization.²³ Furthermore, the unpoled crystal is in possess of domain walls with high density, on which the refractive indices are discontinuous.^{25,26} These domain boundaries lead to multiple scattering and generate larger scattering losses when the incident light passes through the crystal. NBT has high optical loss and low transmittance, which is related to the inhomogeneities over various length scales. However, long range ordered tetragonal phase is enhanced with increasing BT composition,⁵ which contributes to the fact that NBT-6%BT has higher transmission than that of NBT. Whereas, the long-range ordered domains may be broken into some short-range ordered ones as the temperature goes up.¹⁹ The smaller size of the domains and the higher amount of domain walls affect the optical properties, which reduce the overall transmission in the UV/VIS and near-infrared spectral range.²⁷ The absorbance spectra at the wavelength of 650 and 800 nm, defined as $A = -\log_{10} T = \epsilon_2 cd$, are shown in Figs. 4(c) and 4(d), respectively. Here, the coefficient c is the absorbing concentration of crystal, and d is the crystal thickness. Note that the extinction coefficient (ϵ_2) is linear temperature dependent and validated for various types of materials in a large temperature range. Thus, its deviations from a linear fit indicate that structural variations occur in the material.^{27,28} From Figs. 4(c) and 4(d), three deviations

from linearity at 83, 106, and 150 °C are found. These interrupts of slope give evidence for changes of optical properties, which could correspond to the structural variations.

Based on aforementioned discussion, the structural analysis from Raman data relies on discussing soft-mode as a temperature-dependent function of frequency or intensity. What is more, the deviations from a linear fit in spectral absorbance indicate that structural variations occur in the materials. Therefore, the changes in structure of NBT-6%BT crystal are illustrated in both Raman (Fig. 2) and transmittance [Figs. 4(c) and 4(d)] spectra at 106 and 150 °C. In fact, those structural variations, taking place at 106 °C and 150 °C, can be verified. The temperature of 106 °C can be regarded as depolarization temperature of unpoled NBT-6%BT ($T_{d-unpoled}$), which correlates with the structural transition from R3c to P4bm.^{8,11} While the point 150 °C may be associated with FE to anti-ferroelectric transition (AFE) temperature (T_{F-AF}) of NBT-6%BT.^{8,29} In analogy with *in situ* transmission electron microscopy study of NBT-6%BT ceramics,⁸ the textural changes in NBT-6%BT single crystal can be discussed as follow. At RT, the unpoled NBT-6%BT crystal exhibits coexistence of two phase with volumes of R3c ferroelectric domains embedded in the matrix of P4bm nanodomains. During the heating process, the volume with P4bm nanodomains started to grow at the sacrifice of R3c complex ferroelectric domains, which can be viewed as R3c → P4bm transition and correlates with the dielectric anomaly at $T_{d-unpoled}$.⁸ The process continues until about 150 °C on condition that NBT-6%BT crystal completely exhibits the P4bm tetragonal symmetry in the form of nanodomains, which can be regarded as FE to AFE transition for the reason that P4bm is of antiferroelectric nature.⁸ Furthermore, from electrical experiments, in which FE to AFE transition is marked by the onset of dielectric dispersion, T_{F-AF} is also turned out to be ~150 °C.²⁹ It can be concluded that optical behaviors are associated with the structural variations, which has been proved from the abnormally spectra responses observed at 106 and 150 °C in both Raman and absorbance spectra. As for the abnormality in absorbance spectra at 83 °C, it's most related to dipolar freezing temperature (T_{VF}).³⁰ T_{VF} is associated with PNRs in the unpoled specimens. At RT, relaxor NBT-6%BT crystal coexists in PNRs with P4bm and R3c symmetries.^{5,9,12} Below T_{VF} , the PNRs could not grow and coalesce to yield a normal ferroelectric state and the system stays in a dipolar glass state due to the finite coherence length of the out-of-phase octahedral tilt.¹³ When the temperature reaches T_{VF} , the PNRs grow and merge the neighboring PNRs then transform to a normal ferroelectric state, followed thermal evolution of polar nano-regions from R3c to P4bm symmetries. It's worth noting that dielectric anomaly for NBT-*x*%BT at T_{F-AF} is assumed to be attributed to the thermal evolution of these two types of PNRs.⁹ For NBT-6%BT, the system is able to geometrically arrange the PNRs into stripelike domains of increasing length to relax its elastic energy, because the ensemble of polar nano-regions had a notably higher degree of self-organization.⁵ After the transition, NBT-6%BT exhibits the P4bm tetragonal symmetry in the form of nanodomains.

In summary, Raman and ultraviolet-visible spectra of NBT-6%BT single crystal have been investigated. Two

temperature points (106 and 150 °C) concerning the structural changes are found, which can be related to $T_{d-unpoled}$ and T_{F-AF} , respectively. Moreover, it should be noted that there is an abnormality at 83 °C, which is most likely to be associated with thermal evolution of PNRs. It can be confirmed that solid state spectroscopy is an effective tool to study the structural variation of ferroelectric oxides.

One of the authors (T.H.) would like to thank Dr. Xiao Chen for fruitful discussions. This work was financially supported by Major State Basic Research Development Program of China (Grant Nos. 2011CB922200 and 2013CB922300), Natural Science Foundation of China (Grant Nos. 11374097 and 61376129), Projects of Science and Technology Commission of Shanghai Municipality (Grant Nos. 13JC1402100 and 13JC1404200), and the Program for Professor of Special Appointment (Eastern Scholar) at Shanghai Institutions of Higher Learning.

- ¹G. Smolenskii, V. Isupov, A. Agronovskaya, and N. Krainik, *Sov. Phys. Solid State* **2**, 2651 (1960).
- ²Y.-M. Chiang, G. W. Farrey, and A. N. Soukhovjak, *Appl. Phys. Lett.* **73**, 3683 (1998).
- ³T. Takenaka, K. Maruyama, and K. Sakata, *Jpn. J. Appl. Phys.* **30**, 2236 (1991).
- ⁴W. Jo, J. E. Daniels, J. L. Jones, X. L. Tan, P. A. Thomas, D. Damjanovic, and J. Rödel, *J. Appl. Phys.* **109**, 014110 (2011).
- ⁵J. J. Yao, N. Monsegue, M. Murayama, W. N. Leng, W. T. Reynolds, Q. H. Zhang, H. S. Luo, J. F. Li, W. W. Ge, and D. Viehland, *Appl. Phys. Lett.* **100**, 012901 (2012).
- ⁶B. W. Eerd, D. Damjanovic, N. Klein, N. Setter, and J. Trodahl, *Phys. Rev. B* **82**, 104112 (2010).
- ⁷H. Fu and R. E. Cohen, *Nature (London)* **403**, 281 (2000).
- ⁸C. Ma and X. Tan, *J. Am. Ceram. Soc.* **94**, 4040 (2011).
- ⁹W. Jo, S. Schaab, E. Sapper, L. A. Schmitt, H. J. Kleebe, A. J. Bell, and J. Rödel, *J. Appl. Phys.* **110**, 074106 (2011).
- ¹⁰A. Glazer, *Acta Crystallogr.* **28**, 3384 (1972).
- ¹¹C. Ma, X. Tan, E. Dul'kin, and M. Roth, *J. Appl. Phys.* **108**, 104105 (2010).
- ¹²L. A. Schmitt and H. J. Kleebe, *Funct. Mater. Lett.* **3**, 55 (2010).
- ¹³R. Garg, B. N. Rao, A. Senyshyn, P. S. R. Krishna, and R. Ranjan, *Phys. Rev. B* **88**, 014103 (2013).
- ¹⁴X. Chen, Z. G. Hu, Z. H. Duan, X. F. Chen, G. S. Wang, X. L. Dong, and J. H. Chu, *J. Appl. Phys.* **114**, 043507 (2013).
- ¹⁵E. Aksel, J. S. Forrester, B. Kowalski, M. Deluca, D. Damjanovic, and J. L. Jones, *Phys. Rev. B* **85**, 024121 (2012).
- ¹⁶M. K. Niranjana, T. Karthik, S. Asthana, J. Pan, and U. V. Waghmare, *J. Appl. Phys.* **113**, 194106 (2013).
- ¹⁷J. Kreisel, A. M. Glazer, G. Jones, P. A. Thomas, L. Abello, and G. Lucazeau, *J. Phys.: Condens. Matter* **12**, 3267 (2000).
- ¹⁸G. S. Xu, Z. Q. Duan, X. F. Wang, and D. F. Yang, *J. Cryst. Growth* **275**, 113 (2005).
- ¹⁹X. L. Zhang, Z. G. Hu, G. S. Xu, J. J. Zhu, Y. W. Li, Z. Q. Zhu, and J. H. Chu, *Appl. Phys. Lett.* **103**, 051902 (2013).
- ²⁰J. J. Zhu, W. W. Li, G. S. Xu, K. Jiang, Z. G. Hu, M. Zhu, and J. H. Chu, *Appl. Phys. Lett.* **98**, 091913 (2011).
- ²¹S. Trujillo, J. Kreisel, Q. Jiang, J. H. Smith, P. A. Thomas, P. Bouvier, and F. Weiss, *J. Phys.: Condens. Matter* **17**, 6587 (2005).
- ²²R. Migoni, H. Bilz, and D. Bäuerle, *Phys. Rev. Lett.* **37**, 1155 (1976).
- ²³J. Fousek and V. Janovec, *J. Appl. Phys.* **40**, 135 (1969).
- ²⁴C. J. He, L. H. Luo, X. Y. Zhao, H. Q. Xu, X. H. Zhang, T. H. He, H. S. Luo, and Z. X. Zhou, *J. Appl. Phys.* **100**, 013112 (2006).
- ²⁵J. Erhart and W. Cao, *J. Appl. Phys.* **94**, 3436 (2003).
- ²⁶J. Sapriel, *Phys. Rev. B* **12**, 5128 (1975).
- ²⁷H. Katzke, M. Dietze, A. Lahmar, M. Es-Souni, N. Neumann, and S. G. Lee, *Phys. Rev. B* **83**, 174115 (2011).
- ²⁸C. Marin, A. G. Ostrogorsky, G. Foulon, D. Jundt, and S. Motakef, *Appl. Phys. Lett.* **78**, 1379 (2001).
- ²⁹W. W. Ge, C. T. Luo, Q. H. Zhang, C. P. Devreugd, Y. Ren, J. F. Li, H. S. Luo, and D. Viehland, *J. Appl. Phys.* **111**, 093508 (2012).
- ³⁰F. Craciun, C. Galassi, and R. Birjega, *J. Appl. Phys.* **112**, 124106 (2012).